Research Square

Preprints are preliminary reports that have not undergone peer review.
They should not be considered conclusive, used to inform clinical practice,
or referenced by the media as validated information.

A tight inducible model for oncogene function and drug testing

Matthias Hamdorf
University Hospital Bonn
Luca Wallner
University Hospital Bonn
Sonja Sternberg
University Hospital Bonn
Glen Kristiansen
University Hospital Bonn
Verena Tischler
Verena.Tischler@ukbonn.de
University Hospital Bonn

Article

Keywords:

Posted Date: July 31st, 2026

DOI: https://doi.org/10.21203/rs.3.rs-9929991/v1

License: This work is licensed under a Creative Commons Attribution 4.0 International License.
Read Full License

Additional Declarations: No competing interests reported.

Abstract

Precise control of oncogene expression is crucial for advancing tumor biology research and therapeutic testing. To address limitations of current systems, we developed a novel, tightly regulated, genome-integratable inducible expression platform, based on an optimized cumate gene-switch system. By engineering a KRAB-fused, NLS-enhanced CymR repressor (CSwitch-Silencer), a CpG-free hybrid promoter, and a PiggyBac-based integration strategy, insulated by matrix attachment regions, we achieved robust, reversible, and dose-dependent transgene expression with basal activity below detection.

With the receptor tyrosine kinase *cMET* as a model, we generated CRISPR–Cas9-derived *cMET*-deficient A549 cells and established inducible lines expressing wild-type and clinically relevant variants, including exon 14 skipping and H1094Y. The system enabled precise tuning of expression levels and faithful recapitulation of downstream signaling and phenotypic responses. Pharmacological profiling revealed variant-specific sensitivities to clinically relevant MET inhibitors, with the H1094Y mutation exhibiting increased sensitivity to the type II inhibitor cabozantinib, while exon 14 skipping conferred reduced sensitivity. These effects were consistent across biochemical and functional assays, including receptor activation and cell migration.

Collectively, this platform provides a versatile and scalable approach for modeling oncogene function and drug response in a controlled genetic context. Its tight regulation, modular design, and stable genomic integration make it broadly applicable for functional characterization of cancer-associated variants and for preclinical evaluation of targeted therapies.

Introduction

Understanding how oncogenes and tumor suppressors drive tumorigenesis through gain-of-function or loss-of-function mutations is fundamental to improving cancer diagnosis and therapy[1]. A key limitation of many experimental systems is the inability to precisely control the timing, magnitude, and duration of oncogene expression, parameters that critically influence cancer initiation and progression[2]. Inducible expression systems address this limitation by enabling dynamic and reversible gene regulation, thereby providing more physiologically relevant models for studying oncogenic signaling, especially variants of uncertain significance (VUS)[2–4].

Constitutive overexpression and knockdown approaches have been instrumental in identifying cancer drivers[5]. Yet, they often obscure context-dependent effects and fail to recapitulate the transient or graded activation observed in vivo. Inducible systems offer a conceptual and technical advantage by enabling temporal control of gene expression and facilitating the study of dose-dependent phenotypes, oncogene addiction, and therapeutic response[2,6].

Among inducible platforms, the tetracycline-inducible (Tet) system has been the gold standard in this field for decades[7]. In the Tet-On configuration, a reverse tetracycline-controlled transactivator (rtTA) activates transcription upon binding doxycycline. Despite its versatility, this system can exhibit basal leakiness, limited dynamic range[8], and dependence on high transactivator levels, which may confound interpretation in sensitive biological contexts.

An alternative approach is provided by the cumate-inducible system, derived from the *Pseudomonas putida* cym/cmt operons[3,7]. In its repressor configuration, the CymR protein binds to the cumate operator (CuO) sequences and blocks transcription, whereas the addition of cumate induces dissociation and activates gene expression. This system is orthogonal to mammalian regulatory networks, relies on a non-toxic, inexpensive inducer, and provides tight transcriptional control with minimal background activity[3,9].

The versatility of the cumate system has enabled its application in stable, isogenic cancer models, including via lentiviral delivery and targeted genomic integration[2,9]. When combined with genome engineering approaches, inducible systems permit controlled interrogation of oncogene function and drug response in defined genetic backgrounds[7].

Here, we developed an optimized, all-in-one inducible expression system based on a modified CymR repressor fused to a KRAB repression domain, coupled to a CpG-free promoter architecture for the CuO target site. This design achieves near-complete suppression in the uninduced state and robust, cumate-induced, dose-dependent activation. We apply this system to model oncogenic variants of the receptor tyrosine kinase *cMET* in lung cancer cells.

The cellular mesenchymal-epithelial transition factor (cMET) proto-oncogene plays a crucial role in non-small cell lung cancer (NSCLC)[10], and understanding its regulation can significantly impact the development of targeted therapies and diagnostics, emphasizing the importance of our model system.

Among *MET* alterations, exon 14 skipping (cMET ΔEx14) is one of the most common clinically important oncogenic variants[11–14]. This mutation results in loss of the juxtamembrane domain required for Cbl-mediated ubiquitination, receptor degradation, and negative feedback phosphorylation, leading to sustained signaling[12,15,16]. MET ΔEx14 occurs in approximately 2–3% of NSCLC cases[13,14,17,18] and at higher frequencies in specific subtypes, and confers sensitivity to MET tyrosine kinase inhibitors (TKI) such as capmatinib and tepotinib[19,20].

In addition to exon skipping, mutations within the tyrosine kinase domain are increasingly recognized as modulators of oncogenic signaling and therapeutic responses[18,21,22]. The H1094Y substitution, the second most common mutation[23], was initially classified as a variant of uncertain significance. It has been shown to promote proliferation and migration and to function as a resistance mechanism in epidermal growth factor receptor (EGFR) inhibitor-treated tumors[24,25]. Differential sensitivity of such

variants to MET inhibitors underscores the need for controlled model systems to dissect their functional and pharmacological properties.

In our study, we designed an all-in-one transposon vector, highlighting an innovative approach to streamline gene delivery. This provides an advantage to commonly used lentivirus-based systems[2]. We employed a human codon-optimized version of a modified transposase to enhance genomic integration. The hyperactive PiggyBac (hyPB) system is an advanced, non-viral genome engineering tool derived from the natural DNA transposon *PiggyBac*[26]. It has been specifically engineered for superior performance in mammalian cells. The transposase mediates integration via a "cut-and-paste" mechanism, comprising two components of the transposon system: a genetically developed transposase enzyme and a transposon vector. The transposase recognizes specific inverted terminal repeat (ITR) sequences on the vector and precisely excises the transgene, integrating it into "TTAA" chromosomal recognition sites[27].

Here, we present a robust and versatile inducible non-toxic cumate expression system that overcomes key limitations of existing platforms[6]. This system offers a powerful tool for investigating oncogene function, specifically modeling mutation-specific effects of proto-oncogene cMET, and evaluating targeted therapies in a controlled, physiologically relevant preclinical setting, advancing cancer research applications.

Results

Engineering of a tightly regulated inducible oncogene expression system

Initially, we used the commercially available cumate-inducible expression vector from SBI (#PBQM812A-1, Biozol, Eching, Germany (SBI)) and introduced the wildtype cMET gene. Benchmarking the commercial induction cassette in stable cell lines revealed basal leakiness upon puromycin selection and significant loss of induction capacity over four months of culturing (Supplementary Fig. 3A, B). These findings led us to rethink the expression system to meet the need to study oncogenes. To achieve stringent and tunable control of oncogene expression, we developed a compact inducible expression cassette, based on a modified cumate-responsive repressor system. The CymR repressor was fused at its N-terminus to the KRAB-A/B repression domain derived from Kid-1[28], a potent transcriptional silencer homologous to human KRBX5. In addition a simian virus 40 nuclear localization sequence[29] (SV40 NLS) was appended at the C-terminus to ensure efficient nuclear import (Fig. 1A). This engineered repressor, hereafter termed “CSwitch-Silencer”, enables robust transcriptional repression with minimal basal activity (Fig. 3C,D, Supplementary Fig. 5A-C). A T2A self-cleaving peptide was used with the Silencer to simultaneously express puromycin resistance for positive selection after integration into the host genome.

The commercial system used a cytolomegalovirus (CMV)-based promoter. Analysis of these promoters for CpG islands by online prediction tools showed a CpG island region (green marked, supplementary Fig. 3C). These analyses underline the silencing of the inducible promoter over time (Supplementary Fig. 3A, B). In the new system transcriptional regulation was further optimized using a CpG island–free promoter composed of a murine/human CMV enhancer and the human elongation factor 1α (EF1α) promoter to prevent promoter silencing over time[30,31]. One to three cumate operator (CuO) sites were inserted downstream of the promoter and upstream of a short synthetic intron to facilitate repressor binding. In the absence of the inducer, the CSwitch-Silencer efficiently blocks transcription (Fig. 1B, Supplementary Fig. 5, 6), while addition of cumate induces the repressor's dissociation, thereby enabling rapid activation of target gene expression (Fig. 1D, Supplementary Fig. 6A).

Cloning oncogenes, such as cMET downstream of the inducible promoter, enables studying of cMET's role in lung cancer development in a controlled setting and enables further investigation of its role in personalized cancer therapy.

To model clinically relevant alterations, cMET variants were generated by site-directed mutagenesis. These variants included exon 14 skipping, a frequent event in non-small cell lung cancer, and the H1094Y substitution (Fig. 1C). For stable genomic integration, the construct was flanked by PiggyBac inverted terminal repeats (ITR) (Fig. 1D), enabling efficient transposition of the entire cassette. To minimize positional effects, the expression unit was insulated using β-globin and human interferon-β matrix attachment regions (Fig. 1D). To visualize inducability and to positively select inducible cells, we integrated a MintSelect marker (Fig. 1B, C). The selection marker is a fusion of Mint fluorescent protein (MintFP) (human codon optimized LanFP1 with T76V, D156E mutation) to the blasticidin resistance gene (Supplementary Fig. 3A, B).

Generation of cMET-deficient A549 cells

To further investigate cMET function in a defined genetic background, we generated cMET knockout derivatives of the human lung adenocarcinoma cell line A549, which expresses endogenous wild-type cMET. Clustered regularly interspaced short palindromic repeats/CRISPR-associated protein 9 (CRISPR/Cas9)-mediated genome editing using two guide RNAs introduced a 112-bp deletion in the 5' coding region, resulting in a frameshift and a premature stop codon after 35 amino acids (Fig. 2A upper panel).

Single-cell clones were isolated and validated by Sanger sequencing (Fig. 2A lower panel). Two independent knockout clones (B1 and C1) exhibited complete loss of cMET protein expression and abolished receptor activation upon hepatocyte growth factor (HGF) stimulation (Fig. 2B, C). Despite this, no measurable differences in proliferation were observed, consistent with cMET not being a primary driver of cell growth in A549 cells (Supplementary Fig. 1).

We therefore assessed cMET-dependent phenotypes using wound-healing assays. In contrast to wild-type cells, cMET-deficient clones failed to respond to HGF–induced migration (Fig. 2D), demonstrating a critical role for cMET in regulating cell motility in this context.

Generation of inducible cMET variant A549 cell lines

To enable controlled re-expression of cMET variants, the inducible expression cassette was stably integrated into cMET-deficient A549 clones (B1 and C1). Cells were co-transfected with the PiggyBac donor plasmid containing the inducible cassette and a codon-optimized plasmid encoding a hyperactive PiggyBac transposase.

Selection was initiated 96 h post-transfection using puromycin and maintained for 5 days to enrich for successfully transposed cells (Fig. 3A). Surviving cells formed discrete colonies during the selection period (Fig. 3B). To ensure further functional integration of the inducible system, a second selection step for blasticidin resistance conveyed by MintSelect (Supplementary Fig. 2C, D), downstream of the cMET variant, was performed following 48 h of cumate induction, enriching for cells capable of inducible cMET/MintSelect expression. Reporter expression was confirmed by fluorescence imaging (Fig. 3C, Supplementary Fig. 2D).

Following selection, cumate was withdrawn, and cells were expanded to confluency over two weeks to establish stable polyclonal populations. This strategy yielded inducible A549 cell lines suitable for controlling functional interrogation of cMET variants.

Across all cell lines, PiggyBac-mediated integration with cMET variants resulted in the inducible cassette being inserted 4–7 times, as demonstrated by fluorescence in-situ hybridization (FISH) probing for cMET copies (Supplementary Fig. 8, upper panel) and compared to cMET/CEN7 FISH analysis used in molecular diagnostics (Supplementary Fig. 8, lower panel).We next assessed the inducibility and stringency of the system by quantifying fluorescence intensity in uninduced and 48 h induced cells in a 6-well format. Constructs containing a single CuO site exhibited higher maximal reporter expression while maintaining negligible basal activity in the absence of inducer (Fig. 3D). In contrast, constructs with three CuO sites displayed enhanced transcriptional repression, consistent with increased CSwitch-Silencer occupancy, albeit at reduced maximum expression levels (Fig. 3D). Fluorescence imaging of MintFP, with one, two, and three CuO sites, following cumate induction, recapitulated the decrease in gradient MintFP expression with increasing expression control (Supplementary Fig. 4). This configuration is particularly advantageous for the controlled expression of toxic or highly bioactive proteins.

Inducibility and regulatory tightness of all cMET variant cell lines were further validated by immunoblotting and immunohistochemical staining, revealing the abolition of basal leakiness (Supplementary Fig. 5A) and dose-dependent cumate induction of cMET (Supplementary Fig. 5B, C). Moreover, the integrated MintFP signal intensity during 60 h of cumate induction showed linear increase

proportional to cumate concentration (Supplementary Fig. 6A), with the MintFP expression directly correlating with cMET expression. Immunoblotting and quantification yielded a cumate induction power of 81- 86-fold, compared to non-induced at 75 µg/ml (Supplementary Fig. 6B, C). Taken together these findings provide evidence of the system's robustness and reliability for controlled gene expression studies.

Functional validation and pharmacological profiling of cMET variants

To evaluate the utility of this system for therapeutic studies, we assessed the response of inducible cMET variants to clinically relevant inhibitors. Two type Ib inhibitors, i.e. tepotinib and elzovantinib, targeting the ATP-binding pocket of the active receptor conformation[32] and one type II inhibitor, cabozantinib, that additionally engages an allosteric pocket and stabilizes the inactive state[33], were selected (Supplementary Fig. 7A).

All inhibitors effectively suppressed cMET activation at 50–100 nM, as shown by immunoblot analysis (Supplementary Fig. 7B), demonstrating the system's utility for pharmacological profiling and drug sensitivity assessment in cancer research.

To assess downstream functional consequences, we performed wound-healing assays in the presence of inhibitors. The observed effects on cell migration were consistent with the biochemical data (Fig. 4A - C), with the H1094Y variant showing significantly greater sensitivity to cabozantinib compared to wild-type cMET *(*Fig. 4D, E*)*. All inducible cMET variants displayed biological activity, including induction of histomorphological changes consistent with epithelial-to-mesenchymal transition (EMT) (Supplementary Fig. 9).

Methods

Plasmid construction and design of the inducible expression system

The inducible *cMET* expression constructs were derived from the pCMV6-*cMET* plasmid (RC226393, OriGene, Herford, Germany), encoding transcript variant 1 (NM_001127500.1). Initial constructs retaining the native CMV promoter exhibited progressive silencing in A549 cells, consistent with CpG methylation. To overcome this limitation, a CpG-free promoter was engineered by combining a human CMV enhancer with a murine CMV enhancer and the human EF1α promoter.

Cumate operator (CuO) sequences (1X, 2X or 3X) were inserted downstream of the promoter, followed by a synthetic intron to enhance expression. The inducible cassette was flanked by PiggyBac inverted terminal repeats (ITRs) for genomic integration. To insulate the transgene from positional effects, a human β-globin matrix attachment region (MAR) was inserted upstream and an interferon-β S/MAR downstream of the expression cassette.

An all-in-one configuration was generated by incorporating a modified CymR repressor (CSwitch-Silencer) in reverse orientation under control of an EF1α promoter. The CSwitch-Silencer consists of the CymR repressor[3] fused N-terminally to the KRAB-A/B repression domain from Kid-1[28] and C-terminally to an SV40 nuclear localization signal. A puromycin resistance cassette was linked via a T2A peptide[34] to enable bicistronic expression.

All constructs were designed using SnapGene (GSL Biotech LLC, San Diego, USA) and assembled from synthetic DNA fragments (Eurofins Genomics, Ebersberg, Germany) using HiFi DNA Assembly (NEB, Frankfurt, Germany). Assembly was verified by nanopore sequencing (Plasmidsaurus, Köln, Germany).

Generation of the MintSelect reporter construct

To enable visualization and dual selection, a human codon-optimized variant of LanFP1[35] was engineered. Point mutations (T76V and D156E) were introduced using Q5 site-directed mutagenesis (NEB, Frankfurt, Germany) to enhance fluorescence intensity and stability. The resulting protein, termed MintFP, was fused to a blasticidin resistance gene via a short linker to generate the MintSelect cassette.

The MintSelect sequence was inserted downstream of cMET via a T2A peptide, enabling co-expression from a single transcript. Successful expression was confirmed by fluorescence analysis (Supplementary Fig. 2).

Generation of cMET variants

Clinically relevant *cMET* variants were generated by site-directed mutagenesis using the Q5 system (NEB, Frankfurt, Germany). Exon 14 skipping (ΔEx14) and the H1094Y substitution were introduced using mutation-specific primers. All variants were verified by sequencing before functional analysis (Plasmidsaurus, Köln, Germany).

Construction of a hyperactive PiggyBac transposase plasmid

For genomic integration, a codon-optimized hyperactive PiggyBac[26] transposase (hyPBase) was cloned into the pCMV6 backbone by replacing the *cMET* coding sequence using HiFi assembly, generating pCMV6-hyPBase.

Generation of cMET knockout A549 cells

A549 cells (Ubigene, YC-C016, Austin, USA), were edited using CRISPR–Cas9 with two sgRNAs targeting the 5' region of *cMET* (g3: GGT GTT TCC GCG GTG AAG TTG GG; g4: GCC CCC GCT GTG CTT GCA CCT GG). Transfected cells were single-cell cloned and screened by PCR for deletion of a 112 bp fragment.

Genomic DNA was amplified using primer pairs distinguishing wild-type and knockout alleles. Positive clones were confirmed by Sanger sequencing and used for downstream experiments.

Stable integration of inducible constructs

cMET-deficient A549 clones (B1 and C1) were seeded at 0.75 × 10^6 cells per well (6-well format) one day before transfection. Cells were co-transfected with 2 µg PiggyBac donor plasmid, 0.5 µg pCMV-hyPBase, and 0.1 µg pAdVAntage (Promega, Walldorf, Germany) using Lipofectamine 3000 (Thermo Fisher, Dreieich, Germany).

Puromycin selection (6 µg/ml) was initiated 96 h post-transfection and maintained for 5 days. For secondary selection, cells were induced with cumate (75 µg/ml) for 48h and selected with blasticidin (10 µg/ml) for 4 days. Following selection, cells were maintained in the presence of puromycin (4 µg/ml).

Wound-healing assay

Cell migration was assessed using the IncuCyte S3 live-cell imaging system (Satorius, Göttingen, Germany). Cells were seeded in 96-well ImageLock plates (1 × 10^4 cells per well) under reduced serum conditions (1%). Wounds were generated using a WoundMaker device (Satorius, Göttingen, Germany), and cells were treated with or without HGF (50 ng/ml, BioLegend, Koblenz, Germany).

For inhibitor studies, inducible cells were seeded at 3.5 × 10^3 cells per well and induced with cumate (75 µg/ml). Cells were treated with cabozantinib at the indicated concentrations or a DMSO control, followed by wounding and incubation in the presence of HGF and the inhibitor. Images were acquired hourly, and wound closure was quantified using IncuCyte software. Data were analyzed in GraphPad Prism (V10; GraphPad Software, Boston, USA).

Immunoblot analysis

Cells were seeded at 0.75 × 10^6 cells per well and treated with cumate (typically 150 µg/mL; as indicated in the figure) for 48 h. For inhibitor studies, cells were serum-reduced and treated with inhibitors before HGF stimulation (50 ng/ml, 10 min).

Cells were lysed in LDS sample buffer, and proteins were separated on 4–12% Bis-Tris gels and transferred to nitrocellulose membranes. Membranes were blocked and probed with antibodies against phospho-cMET (Tyr1234/1235) (3D7, Cell Signaling, Frankfurt, Germany), total cMET (AB227637, Abcam, Cambridge, UK), and β-actin (W16197A, BioLegend, Koblenz, Germany). HRP-conjugated secondary antibodies were used (Cytiva NA9340, Merck, Darmstadt, Germany), and signals were detected using enhanced chemiluminescence and imaged on a ChemiDoc system (Bio-Rad, Feldkirchen, Germany). Densitometric analysis was performed with Fiji[36].

Fluorescence in-situ hybridization

The *MET* hybridization probe was generated by excising the full-length *MET* coding sequence (4224 bp), which was fluorescently labeled with the Atto488 NT Labeling Kit following the manufacturer's

instructions (Jena Bioscience, Jena, Germany). Cells were seeded on slides 24 h before paraformaldehyde fixation (4%, 10 min). Triton-X was used to permeabilize the cells, followed by dehydration with 70, 85, and 100 percent ethanol. Slides were air-dried before hybridization. Tumor cell nuclei were analyzed using fluorescence microscopy (Leica DM 6000, Leica Microsystems, Wetzlar, Germany) and images were captured with Diskus software (Carl H. Hilgers, Koenigswinter, Germany).

Discussion

Precise control of oncogene expression is essential for dissecting the functional impact of driver mutations and variants of uncertain significance (VUS), and for evaluating preclinical therapeutic responses in a physiologically relevant context. Although a range of inducible systems is commercially available[7], we found that existing platforms did not meet key experimental requirements, including minimal basal expression, sustained activity following genomic integration, and robust inducibility[7]. Limitations such as transcriptional leakiness[37], CpG methylation–mediated silencing[38], incomplete genomic integration, and restricted dynamic range frequently compromised their utility.

To address these challenges, we developed a fully integrated, all-in-one inducible expression system that combines stringent transcriptional control with stable genomic insertion. The system is based on the cumate gene-switch architecture[3], which we further optimized to enhance repression and reduce background activity. Specifically, fusion of the CymR repressor to a KRAB-A/B domain[39] and the addition of a strong SV40 nuclear localization signal markedly improved transcriptional silencing (Fig. 1A, 3C, D).In comparison to the commercially available system from SBI, our system showed advanced tightness and no CpG silencing (Supplementary Fig. 3A -B, 5A – C and 6A -C).

In parallel, we replaced conventional CMV-based promoters, which are prone to CpG methylation and silencing[38], with a CpG-free hybrid promoter (Fig. 3C) composed of murine and human CMV enhancers linked to an EF1α core promoter (Fig. 1B). Our vector system addresses key limitations of conventional lentiviral approaches[2], which typically require integrating multiple independent vectors and are limited in the size of the integrated information. The ratio of repressor to inducible cassettes is critical for tight control and strongly depends on the multiplicity of infection (MOI) in lentiviral transduction. By consolidating all components necessary for inducible gene regulation into a single genomic locus, our system ensures coordinated integration and enforces a defined expression stoichiometry; the only limitation of the integration length is given by the bacteria used for the plasmid amplification. Integration of the inducible cassette together with the CSwitch-Silencer into a PiggyBac transposon framework[26], flanked by matrix attachment regions, ensured stable genomic insertion and minimized positional effects (Fig. 1D, Supplementary Fig. 8)[40]. This design minimizes variability arising from positional effects and heterogeneous copy numbers, which are common challenges in multi-vector systems[41].

Stable genomic incorporation of inducible systems remains a challenge in the field. While a variety of inducible platforms have been developed, their long-term functionality is frequently compromised after

chromosomal integration, often due to epigenetic silencing or imbalanced expression of components[30,31]. In our study, cell lines generated with this system maintained consistent performance and remained robust across multiple freeze–thaw cycles. This stability likely reflects both the single-locus integration strategy and the inclusion of a synthetic CpG fusion promoter, which may contribute to sustained transcriptional activity.

These modifications further improved system fidelity, and the engineered CSwitch-Silencer reduced basal expression to levels below the limit of detection (Supplementary Fig. 5B, C). Through a combination of promoter optimization and enhanced repressor function, tightened transcriptional control was achieved. Our approach builds on the extensively characterized tetracycline-inducible system, leveraging its modularity while addressing known limitations in background activity. Recent developments, including promoter refinements such as pTRE3G and systems incorporating additional translational control layers (e.g., CASwitch), similarly aim to suppress leakiness[42]. While these strategies have demonstrated improvements, a systematic, side-by-side comparison across platforms remains lacking.

This configuration yielded a tightly regulated and reversible system with negligible basal expression and robust, dose-dependent inducibility (Fig. 3d, Supplementary Fig. 5B). The incorporation of one or multiple cumate operator sites enabled tuning between maximal expression output and enhanced repression, providing flexibility depending on the biological context[9] (Fig. 1B, 3C, 4D, Supplementary Fig. 4). The addition of the MintSelect reporter further enabled direct visualization and dual selection of transgene-expressing cells (Supplementary Fig. 2A -D).

We applied this system to study the receptor tyrosine kinase cMET, a key oncogenic driver in non-small cell lung cancer[10]. Using CRISPR–Cas9, we established *cMET*-deficient A549 cells, providing a controlled background for re-expression studies (Fig. 2A - D). Introduction of wild-type and mutant *cMET* variants, including exon 14 skipping[15] and H1094Y[21] (Fig. 1C, Supplementary Fig. 6B), enabled direct comparison of their functional and pharmacological properties (Fig. 4, Supplementary Fig. 7) under tightly controlled expression conditions (Fig. 1D, Supplementary Fig. 5B, C).

Pharmacological profiling demonstrated that both type I and type II *cMET* inhibitors (Supplementary Fig. 7A) effectively suppressed receptor activation at higher concentrations (Supplementary Fig. 7B)[21,43,44]. However, dose–response analyses revealed variant-specific differences: the H1094Y mutation showed increased sensitivity to the type II inhibitor cabozantinib, whereas the exon 14–skipping variant exhibited reduced sensitivity (Fig. 4A-C). Functional assays assessing cell migration were consistent with these biochemical findings, confirming that the inducible system faithfully recapitulates downstream phenotypic effects of *cMET* signaling in migration and its inhibition (Fig. 4D, E) or EMT (Supplementary Fig. 9). Strong overexpression and activation of cMET and variants are leading to lengthening of the cells and transformation of the shape (Supplementary Fig. 9B). These results are in line with the findings of Liu at al. showing cMET driven EMT[45]. Notably, the increased sensitivity of H1094Y to cabozantinib contrasts with observations in murine Ba/F3 models, where reduced sensitivity

has been reported[21]. This discrepancy emphasizes the importance of cellular context and underscores the need for human, tissue-relevant model systems when evaluating oncogene function and drug response. The ability of the present system to operate in a human cancer cells, in contrast to murine models (e.g. Ba/F3) and the mutational background of cancer cell lines, with tight expression control provides a distinct advantage for such analyses.

Beyond *cMET*, the modular design of this platform enables its application to a wide range of oncogenes and tumor suppressors. The combination of tight repression, tunable induction, stable genomic integration, and dual selection makes it particularly well suited for studying genes with strong or toxic phenotypes, as well as for systematic functional characterization of emerging cancer-associated variants.

In summary, we present a robust and versatile inducible expression system that overcomes key limitations of existing expression systems. We provide a powerful tool for investigating oncogene functions, modeling mutation-specific effects, and evaluating targeted therapies in a controlled and physiologically relevant setting. Our system combines low basal activity with robust, dose-dependent induction. Its simplified genomic architecture and sustained long-term performance make it tailored for translational applications requiring precise and stable gene regulation. Future work should focus on benchmarking against existing systems and exploring its utility across diverse cellular models and biological contexts.

Declarations

Funding Declaration

This research received no specific grant from any funding agency in the public, commercial, or not-for-profit sectors.

Author Contribution

V. T. and M. H. designed and conceptualized the work; M. H., L. W., and S. S. acquisited the data. M. H., L. W. , and S. S. analyzed the data. M. H., L. W., and V. T. interpreted the data; M. H., G. K., and V. T. have drafted and revised the manuscript. All authors have approved the submitted version and agreed both to be personally accountable for the author's own contributions and to ensure that questions related to the accuracy or integrity of any part of the work, even ones in which the author was not personally involved, are appropriately investigated, resolved, and the resolution documented in the literature.

Acknowledgement

Special thanks to Prof. Dr. Hubert Schorle and Dr. José Alberto Rodríguez Castillo for helpful scientific discussions and revision of the manuscript.This research received no specific grant from any funding agency in the public, commercial, or not-for-profit sectors.

Data Availability

All data supporting the findings of this study are available within the paper and its Supplementary Information.

References

1. Morris, L. G. T. & Chan, T. A. Therapeutic targeting of tumor suppressor genes. *Cancer* **121**, 1357–1368 (2015).
2. Kent, M. R., Jay, A. N. & Kendall, G. C. New dual inducible cellular model to investigate temporal control of oncogenic cooperating genes. *Sci. Rep.* **14**, 20773 (2024).
3. Mullick, A. et al. The cumate gene-switch: a system for regulated expression in mammalian cells. *BMC Biotechnol.* **6**, 43 (2006).
4. Goverdhana, S. et al. Regulatable Gene Expression Systems for Gene Therapy Applications: Progress and Future Challenges. *Mol. Ther. J. Am. Soc. Gene Ther.* **12**, 189–211 (2005).
5. Gonzalez-Salinas, F., Martinez-Amador, C. & Trevino, V. Characterizing genes associated with cancer using the CRISPR/Cas9 system: A systematic review of genes and methodological approaches. *Gene* **833**, 146595 (2022).
6. Ansari, M. A., Sharma, R., Swami, P. & Rode, A. B. Small Molecule-Based Conditional Gene Regulation: Advances and Applications. *Chemistry–Methods* **6**, e202500137 (2026).
7. Kallunki, T., Barisic, M., Jäättelä, M. & Liu, B. How to Choose the Right Inducible Gene Expression System for Mammalian Studies? *Cells* **8**, 796 (2019).
8. Agha-Mohammadi, S. et al. Second-generation tetracycline-regulatable promoter: repositioned tet operator elements optimize transactivator synergy while shorter minimal promoter offers tight basal leakiness. *J. Gene Med.* **6**, 817–828 (2004).
9. Xie, J. et al. Development and Application of a Cumate-Inducible Promoter, P gc, in Komagataella pastoris. *Microb. Biotechnol.* **19**, e70311 (2026).
10. Tsao, M. S. et al. MET (c-Met) protein overexpression is an emerging protein biomarker in non-small cell lung cancer. *Npj Precis Oncol.* **9**, 369 (2025).
11. Liang, H. & Wang, M. M. E. T. Oncogene in Non-Small Cell Lung Cancer: Mechanism of MET Dysregulation and Agents Targeting the HGF/c-Met Axis. *OncoTargets Ther.* **13**, 2491–2510 (2020).
12. Cortot, A. B. et al. Exon 14 Deleted MET Receptor as a New Biomarker and Target in Cancers. *JNCI J. Natl. Cancer Inst.* **109**, djw262 (2017).

13. Frampton, G. M. et al. Activation of MET via Diverse Exon 14 Splicing Alterations Occurs in Multiple Tumor Types and Confers Clinical Sensitivity to MET Inhibitors. *Cancer Discov*. **5**, 850–859 (2015).
14. Mazieres, J. et al. MET Exon 14 Skipping in NSCLC: A Systematic Literature Review of Epidemiology, Clinical Characteristics, and Outcomes. *Clin. Lung Cancer* 24, 483–497 (2023).
15. Van Der Steen, N. et al. cMET Exon 14 Skipping: From the Structure to the Clinic. *J. Thorac. Oncol.* **11**, 1423–1432 (2016).
16. Bahcall, M. et al. Combination of Type I and Type II MET Tyrosine Kinase Inhibitors as Therapeutic Approach to Prevent Resistance. *Mol. Cancer Ther.* **21**, 322–335 (2022).
17. Socinski, M. A., Pennell, N. A. & Davies, K. D. MET Exon 14 Skipping Mutations in Non–Small-Cell Lung Cancer: An Overview of Biology, Clinical Outcomes, and Testing Considerations. *JCO Precis Oncol.* 653–663. 10.1200/PO.20.00516 (2021).
18. Ji, M., Ganesan, S., Xia, B. & Huo, Y. Targeting c-MET Alterations in Cancer: A Review of Genetic Drivers and Therapeutic Implications. *Cancers* **17**, 1493 (2025).
19. Drusbosky, L. M., Dawar, R., Rodriguez, E. & Ikpeazu, C. V. Therapeutic strategies in METex14 skipping mutated non-small cell lung cancer. *J. Hematol. Oncol. J. Hematol. Oncol.* **14**, 129 (2021).
20. Wolf, J. et al. Capmatinib in MET Exon 14–Mutated or MET-Amplified Non–Small-Cell Lung Cancer. *N Engl. J. Med.* **383**, 944–957 (2020).
21. Pecci, F. et al. Activating Point Mutations in the MET Kinase Domain Represent a Unique Molecular Subset of Lung Cancer and Other Malignancies Targetable with MET Inhibitors. *Cancer Discov*. **14**, 1440–1456 (2024).
22. Rivas, S. et al. MET Exon 14 Skipping and Novel Actionable Variants: Diagnostic and Therapeutic Implications in Latin American Non-Small-Cell Lung Cancer Patients. *Int. J. Mol. Sci.* **25**, 13715 (2024).
23. Estevam, G. O. et al. Mapping kinase domain resistance mechanisms for the MET receptor tyrosine kinase via deep mutational scanning. *eLife* **13**, RP101882 (2025).
24. Medová, M. et al. The Novel ATP-Competitive Inhibitor of the MET Hepatocyte Growth Factor Receptor EMD1214063 Displays Inhibitory Activity against Selected MET-Mutated Variants. *Mol. Cancer Ther.* **12**, 2415–2424 (2013).
25. Aggarwal, V. & Kim, C. EP.12A.39 MET Point Mutations as the Mechanism of Resistance to EGFR-TKI Therapy: A Case Report of MET H1094Y-Mediated Resistance to Osimertinib Overcome by Capmatinib and a Systematic Review. *J. Thorac. Oncol.* **19**, 637 (2024).
26. Yusa, K., Zhou, L., Li, M. A., Bradley, A. & Craig, N. L. A hyperactive piggyBac transposase for mammalian applications. *Proc. Natl. Acad. Sci. U. S. A.* 108, 1531–1536 (2011).
27. Zhao, S. et al. PiggyBac transposon vectors: the tools of the human gene encoding. *Transl Lung Cancer Res.* **5**, 120–125 (2016).
28. Witzgall, R., O'Leary, E., Leaf, A., Onaldi, D. & Bonventre, J. V. The Krüppel-associated box-A (KRAB-A) domain of zinc finger proteins mediates transcriptional repression. *Proc. Natl. Acad. Sci.* 91, 4514–

4518 (1994).
29. Garcia-Bustos, J., Heitman, J. & Hall, M. N. Nuclear protein localization. *Biochim Biophys. Acta BBA - Rev Biomembr*. **1071**, 83–101 (1991).
30. Zimak, J. et al. Epigenetic silencing directs expression heterogeneity of stably integrated multi-transcript unit genetic circuits. *Sci. Rep.* **11**, 2424 (2021).
31. Cabrera, A. et al. The sound of silence: Transgene silencing in mammalian cell engineering. *Cell. Syst.* **13**, 950–973 (2022).
32. Collie, G. W. et al. Structural and Molecular Insight into Resistance Mechanisms of First Generation cMET Inhibitors. *ACS Med. Chem. Lett.* **10**, 1322–1327 (2019).
33. Damghani, T., Elyasi, M., Pirhadi, S., Haghighijoo, Z. & Ghazi, S. Type II C-met inhibitors: molecular insight into crucial interactions for effective inhibition. *Mol Divers* **26**, (2022).
34. Hurh, S. et al. Expression analysis of combinatorial genes using a bi-cistronic T2A expression system in porcine fibroblasts. *PloS One*. **8**, e70486 (2013).
35. Baumann, D. et al. A family of GFP-like proteins with different spectral properties in lancelet Branchiostoma floridae. *Biol. Direct*. **3**, 28 (2008).
36. Schindelin, J. et al. Fiji: an open-source platform for biological-image analysis. *Nat. Methods*. **9**, 676–682 (2012).
37. Ede, C., Chen, X., Lin, M. Y. & Chen, Y. Y. Quantitative Analyses of Core Promoters Enable Precise Engineering of Regulated Gene Expression in Mammalian Cells. *ACS Synth. Biol.* **5**, 395–404 (2016).
38. Brooks, A. R. et al. Transcriptional silencing is associated with extensive methylation of the CMV promoter following adenoviral gene delivery to muscle. *J. Gene Med.* **6**, 395–404 (2004).
39. Urrutia, R. KRAB-containing zinc-finger repressor proteins. *Genome Biol.* **4**, 231 (2003).
40. Wang, X. J. et al. Sus scrofa matrix attachment region enhances expression of the PiggyBac system transfected into HEK293T cells. *Biotechnol. Lett.* **38**, 949–958 (2016).
41. Grandchamp, N. et al. Influence of insulators on transgene expression from integrating and non-integrating lentiviral vectors. *Genet. Vaccines Ther.* **9**, 1 (2011).
42. Engineering a synthetic. gene circuit for high-performance inducible expression in mammalian systems |. *Nat. Commun.* https://www.nature.com/articles/s41467-024-47592-y
43. Albers, J. et al. The Preclinical Pharmacology of Tepotinib—A Highly Selective MET Inhibitor with Activity in Tumors Harboring MET Alterations. *Mol. Cancer Ther.* **22**, 833–843 (2023).
44. Yakes, F. M. et al. Cabozantinib (XL184), a Novel MET and VEGFR2 Inhibitor, Simultaneously Suppresses Metastasis, Angiogenesis, and Tumor Growth. *Mol. Cancer Ther.* **10**, 2298–2308 (2011).
45. Liu, F. et al. HGF induces EMT in non-small-cell lung cancer through the hBVR pathway. *Eur. J. Pharmacol.* **811**, 180–190 (2017).

Figures

Figure 1

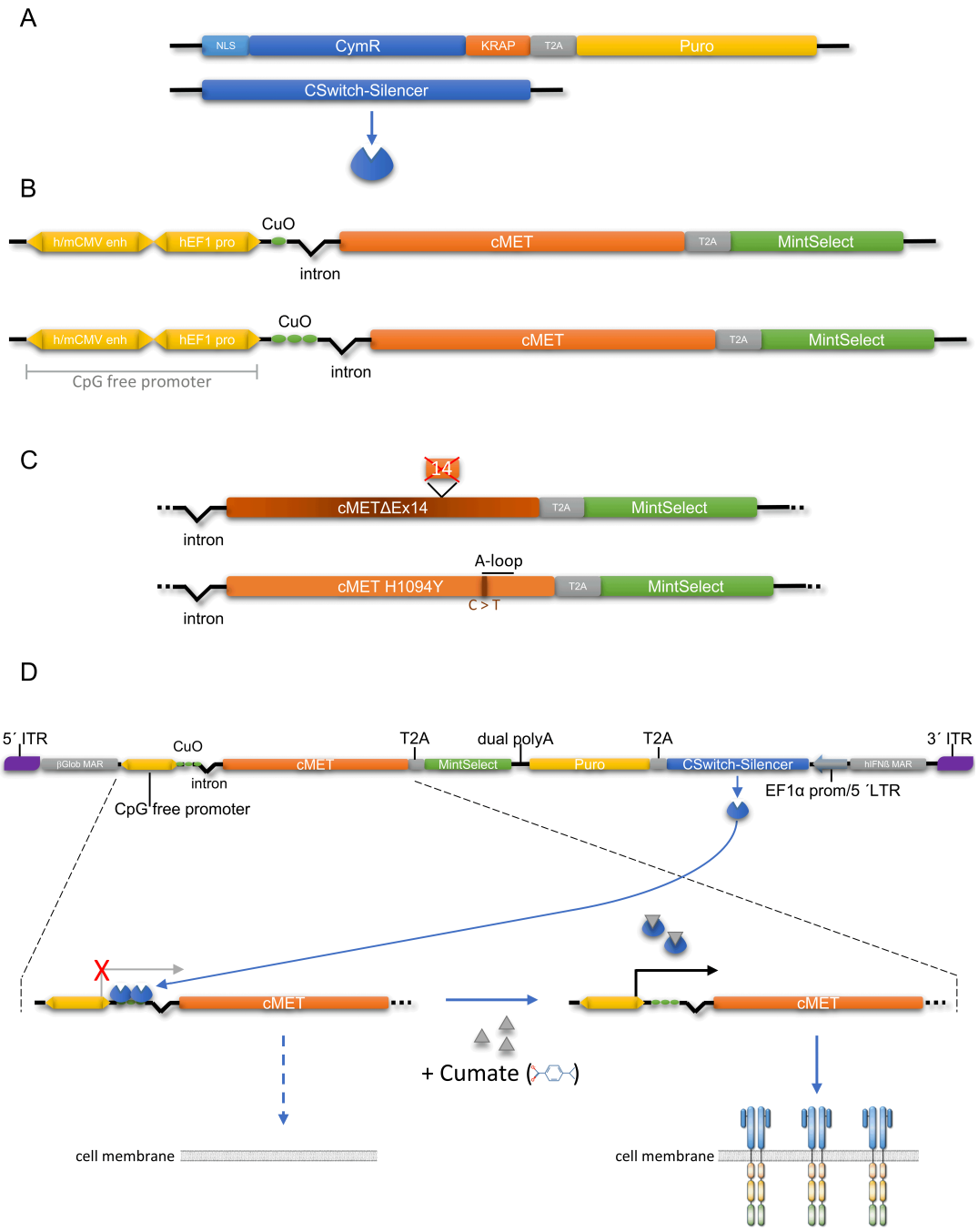


Figure 1

Construction of a genome-integratable, cumate-inducible expression system.

A, Schematic of the CSwitch-Silencer, an NLS-enhanced fusion protein comprising CymR and the KRAB A/B silencer domain.

B, Schematic of CpG-free promoters containing one (1×) or three (3×) cumate operator (CuO) sites, enabling combined expression of cMET WT and the MintSelect selection marker.

C, Schematic representation of two common NSCLC-associated cMET alterations, cMET ΔEx14 and cMET H1094Y.
D, Overview of the complete PiggyBac-based, genome-integratable cumate-inducible expression system. ITR, inverted terminal repeats; S/MAR, scaffold/matrix attachment region; CuO, cumate operator.

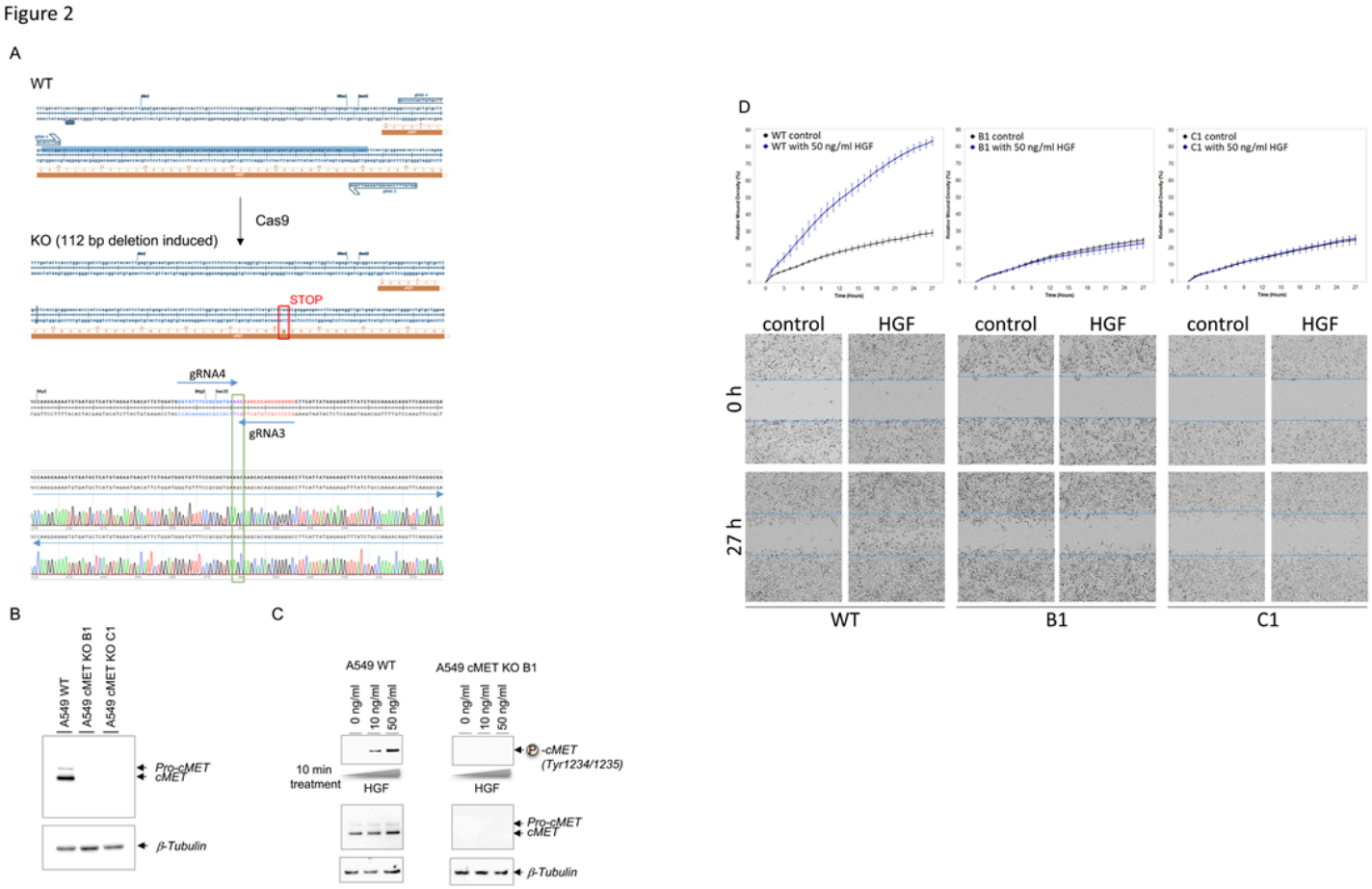


Figure 2

Generation and validation of cMET knockout A549 cells.
A, Guide RNA (gRNA) design targeting the coding region of cMET. The expected 112-bp deletion is indicated (blue), resulting in a frameshift and premature stop codon (red box).
B, Sanger sequencing analysis of selected clones (B1 and C1) confirming biallelic editing (representative forward and reverse traces for clone C1 shown).
C, Immunoblot validation of cMET loss in knockout clones. Original blots of the cropped blots are presented in Supplementary Figure 10.
D, Functional validation of WT and knockout cells by stimulation with hepatocyte growth factor (HGF) and assessment of cMET phosphorylation; knockout cells (clone B1 shown) lack responsiveness. Original blots of the cropped blots are presented in Supplementary Figure 10.
E, Cell migration (wound-healing) assay demonstrating loss of HGF-induced migration in knockout clones compared to WT cells.

Figure 4

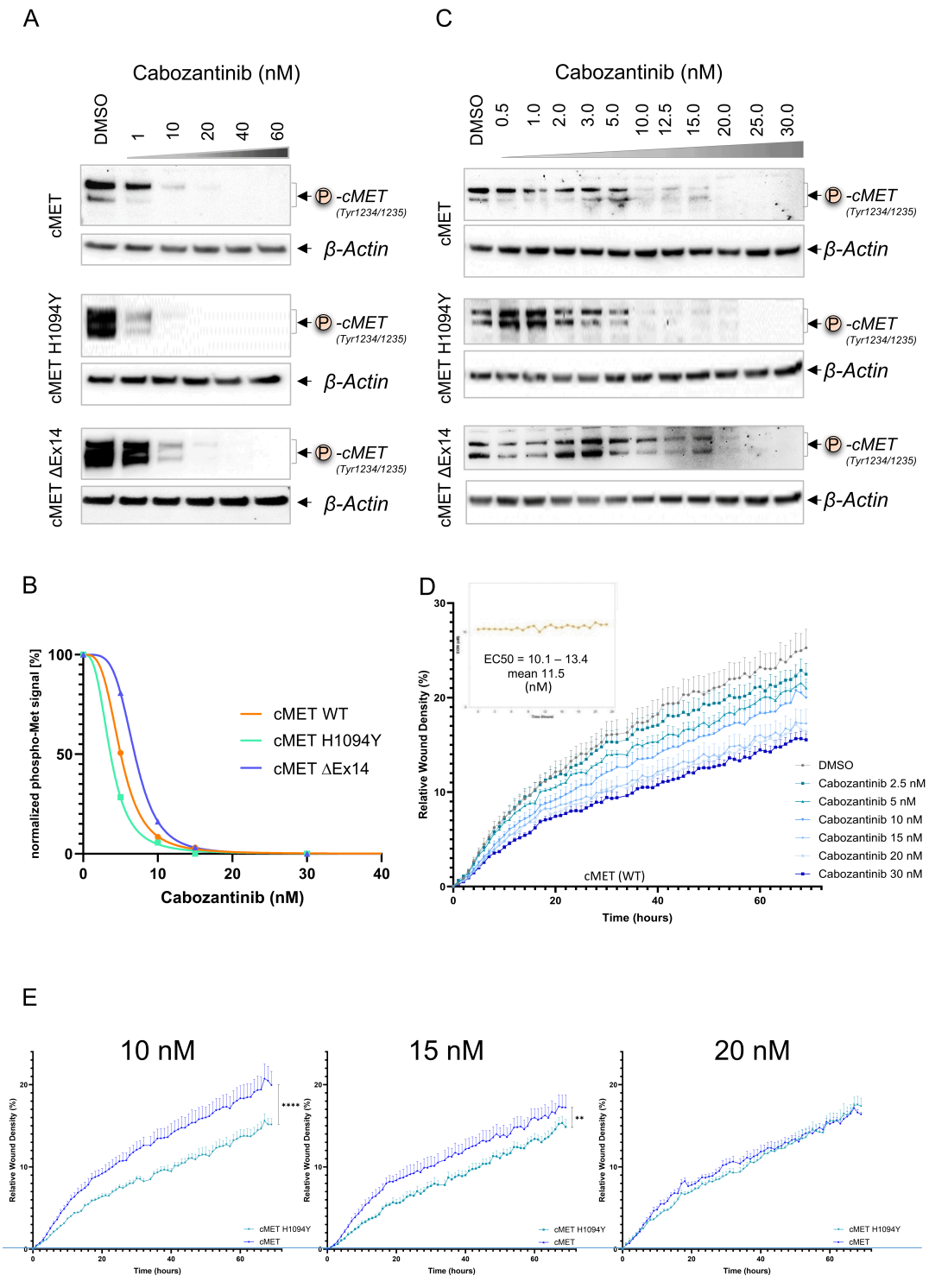


Figure 3

Evaluation of the inducible system for testing cMET inhibitors.

A, Immunoblot analysis of inducible cMET WT, ΔEx14 and H1094Y cell lines treated with increasing concentrations of the type II inhibitor cabozantinib (broad range), followed by HGF stimulation (50 ng/ml) and assessment of cMET phosphorylation. Original blots of the cropped blots are presented in Supplementary Figure 12.

B, As in a, using a narrower concentration range of cabozantinib. Original blots of the cropped blots are presented in Supplementary Figure 13.

C, Functional assessment of inhibitor response by wound-healing assay with live-cell imaging (IncuCyte) over 72 h. ED_{50}values were calculated at each time point (cMET WT shown as example; n = 3, with four technical replicates).

D, Comparison of migration between inducible cMET WT and H1094Y cells; statistical significance determined by one-way ANOVA.

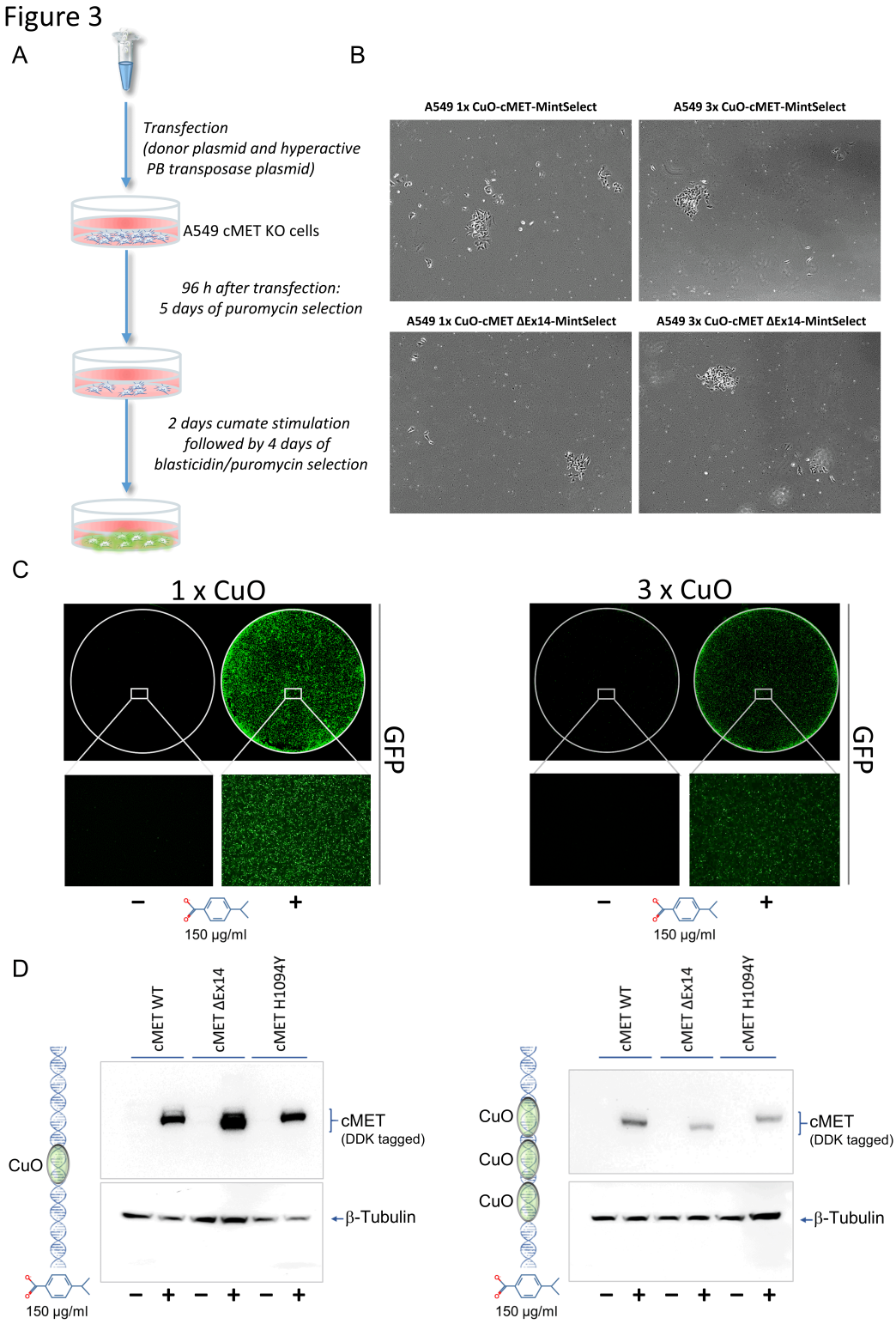


Figure 4

Generation and validation of inducible cMET-expressing cell lines.
A, Schematic overview of the transfection and selection workflow for engineering inducible cell lines.
B, Representative images of puromycin-selected colonies expressing cMET WT or cMET ΔEx14 under 1× or 3× CuO promoters.
C, Validation of inducible co-expression of cMET and MintSelect. Representative stitched images of full 6-well plates ± cumate (40X; Keyence BZ-X800) comparing 1× and 3× CuO constructs (n = 3).
D, Immunoblot analysis comparing inducibility and basal expression of 1× and 3× CuO systems. Original blots of the cropped blots are presented in Supplementary Figure 11

Supplementary Files

This is a list of supplementary files associated with this preprint. Click to download.

- Supplementaryfigures.pdf
- SupplementaryInfo.docx